Available online at www.sciencedirect.com
ScienceDirect
Coastal Engineering 55 (2008) 261–275
Coastal Engineering
An International Journal for Coastal, Harbour and Offshore Engineers
www.elsevier.com/locate/coastaleng

Effective fetch and non-linear four-wave interactions during wave growth in slanting fetch conditions

Marcel Bottema [a,1], Gerbrant van Vledder [b,c,*]

[a] Institute for Inland Water Management and Waste Water Treatment: Rijkswaterstaat/RIZA PO Box 17, 8200 AA Lelystad The Netherlands
[b] Alkyon Hydraulic Consultancy and Research, PO Box 248, 8300 AE Emmeloord The Netherlands
[c] Delft University of Technology, P.O. Box 5048, 2600 GA, Delft, The Netherlands

Received 24 November 2006; received in revised form 6 October 2007; accepted 6 November 2007
Available online 11 December 2007

Abstract

Wave growth in slanting fetch (with wind blowing obliquely off a coast) is investigated with 7 years worth of routine wave measurements in Lake IJssel in The Netherlands and with the SWAN wave model. Two aspects are considered in particular for this case: the validity of the concept of effective fetch and the role of the non-linear four-wave interactions. For slanting and parallel fetch conditions, we found some significant deviations from the effective fetch assumption, leading to 20–35% mismatch in either the peak period T_p or the significant wave height H_{m0} respectively. However, the effect of discrepancies between various widely accepted wave growth formulas turned out to be even more important. The wave directions during slanting fetch are significantly 'steered' by the coastline, especially in the first kilometre(s) off the coast. The role of the non-linear four-wave interactions is investigated by running the SWAN (version 40.41) wave model with three different quadruplet formulations. Exact quadruplet methods (Xnl) yielded relatively strong wave steering, despite the four-wave interactions being relatively weak. Application of Xnl did not lead to better overall agreement with measurements — improvements for the mean wave period T_{m01} were offset by some deterioration for the wave height H_{m0}.

Keywords: Waves; Wave growth; Wave measurements; SWAN; DIA; Xnl

1. Introduction

A special case of finite-fetch wave growth is the case of slanting fetch, when the wind blows obliquely from the shore, rather than perpendicularly. Both experimental studies (e.g., Holthuijsen, 1983; Donelan et al., 1985; Pettersson, 2004) and modelling studies (Bottema and Van Vledder, 2005; Ardhuin et al., 2006) have shown that in cases with slanting fetch, the dominant wave direction may significantly deviate from the wind direction. Directional wave spectra are also influenced as low-frequency components tend to be largely alongshore, while wave components well above the peak frequency tend to be aligned with the wind (Ardhuin et al., 2006).

Throughout the last decades, various modelling approaches have been used to model wave growth in slanting fetch conditions, such as:

- wave modelling with parametric wave growth formulas.
- directionally decoupled wave modelling.
- full spectral wave modelling.

The use of parametric wave growth formulas is convenient and computationally cheap, but it relies on the assumption that cases with complex shorelines can be translated to equivalent cases with straight shorelines, shore-normal wind and a so-called 'effective fetch' that accurately predicts the wave heights and periods at the location of interest. The formulas of Bretschneider CERC, 1984, Kahma and Calkoen (1992), and Young and Verhagen (1996) are examples of the basic formulas used for this first approach. Seymour (1977) proposed a

* Corresponding author. Tel.: +31 527 248100.
E-mail addresses: Marcel_._Bottema@rws.nl (M. Bottema), vledder@alkyon.nl (G.Ph. van Vledder).
[1] Tel.: +31 320 298898.

0378-3839/$ - see front matter © 2007 Elsevier B.V. All rights reserved.
doi:10.1016/j.coastaleng.2007.11.001

directionally decoupled approach as an alternative for the straightforward use of parametric wave growth formulas. Essentially, wave components are evaluated separately for each wave direction, and then added. In this way, an important phenomenon of waves in slanting fetch could be reproduced: the fact that mean wave directions are not fully along wind, as they are partly steered by the shoreline (Holthuijsen, 1983; Donelan et al., 1985). Examples of this second approach are the model of Seymour (1977) and the HISWA model of Holthuijsen et al. (1989). However, Pettersson (2004) suggested that the directionally decoupled approach is not fully adequate: non-linear four-wave interactions (henceforth 'quadruplet interactions') also play a key role in the prediction of alongshore wave steering in slanting fetch conditions since they transfer energy between wave components with different directions. As a result, a full spectral approach including quadruplet interactions would be required. The SWAN wave model (Booij et al., 1999) is such a model and it is specifically designed for small-scale applications on scales of roughly 0.3–300 km and is an example of the full spectral approach. Despite significant improvements in modelling technology (Ardhuin et al., 2006), the physical mechanisms behind wave growth in slanting fetch do not yet seem to be fully clear. As a result, there are also some uncertainties about the general modelling approach that is to be preferred.

So far the scientific interest of wave growth in slanting fetch. The practical interest of this phenomenon is related to ship traffic and flooding prevention. As for the ship traffic, ships prefer to travel along the wave direction — if this is not possible due to for example mixed seas, this can contribute to uncomfortable or even dangerous sea states (Toffoli et al., 2004). Such conditions may occur when ships enter or leave a harbour during slanting fetch, as low-frequency wave components then tend to propagate along the coast, rather than along the wind (Pettersson, 2004; Ardhuin et al., 2006; Bottema and Van Vledder, 2005). Although such sea states are not exceptionally high, it must be taken into account that many ships in the present region of interest (Lake IJssel in the Netherlands, Fig. 1) are designed for inland waters only.

As for the aspect of flooding prevention, historical sources (summarized by Flameling, 2003) suggest that during the 1953 flooding disaster, many dike breaches in the Rhine–Scheldt–Meuse estuary occurred at locations, which must have been relatively sheltered from the wind and the waves. In the 1916 disaster, several dike breaches occurred along the former 'Zuiderzee' estuarine area. In this case, a dike breach at a relatively sheltered location contributed to the flooding of the 'Waterland' region immediately Northeast of the city of Amsterdam. Given these historical dike breaches at sheltered – and therefore somewhat unexpected – locations, it is certainly worth to investigate the phenomenon of wave growth in slanting fetch conditions. This is all the more so because the waves in slanting fetch conditions are considerably higher than in situations with the wind blowing perpendicularly off the coast (Bottema and Van Vledder, 2005).

A final practical issue is related to the current practice of probabilistic evaluation of dike design conditions for the Lake IJssel area in the Netherlands. For this probabilistic evaluation, at least 540 different combinations of wind, lake water levels and river discharges (into Lake IJssel) have to be considered. Therefore, operational requirements (viz. small computing times) are nearly as important for the underlying wave models as the general accuracy of these models.

The latter issue brings us to the main research question of this paper: *Which general modelling principle is most suitable in slanting fetch conditions*: parametric wave growth curves, a

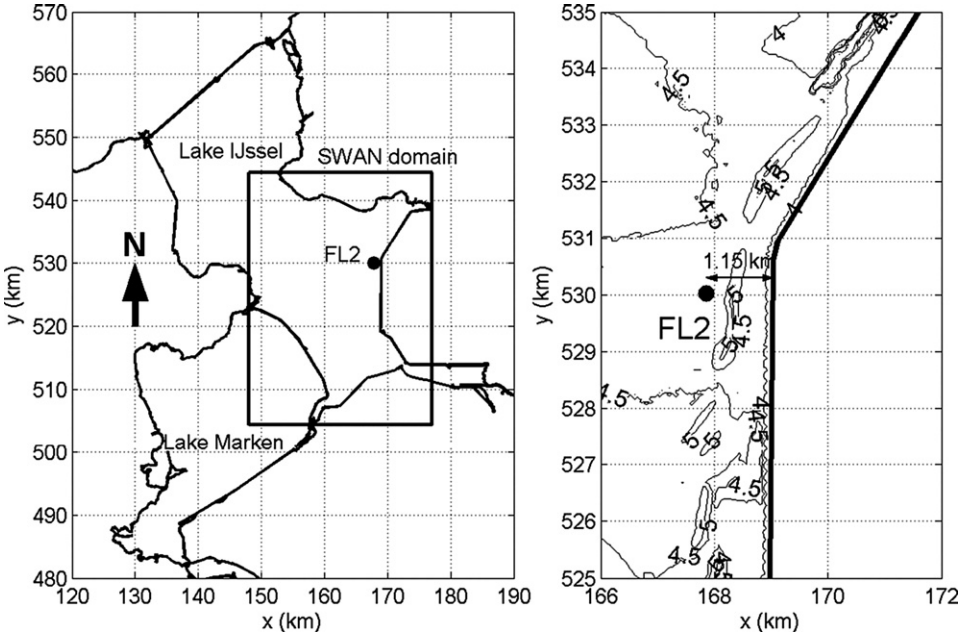

Fig. 1. Lake IJssel, measurement location FL2 and the SWAN model domain (the rectangular box) and detail of bottom topography around location FL2.

directionally decoupled approach, or a full spectral wave model. It should be noted that this paper addresses only one of the wave modelling issues relevant to dike design near Lake IJssel. For problems related to depth-limited (rather than fetch-limited) wave growth and for general model validation results, the reader is referred to De Waal (2001) and Bottema et al. (2003) respectively. Also, it is important to note that it is not the aim of this paper to validate specific wave models and their tunings. Rather, it is the aim to investigate the validity of two underlying key assumptions:

- the validity of the effective fetch concept in slanting fetch, in relation to the use of parametric wave growth curves.
- the role of the quadruplet interactions in slanting fetch, in relation to the choice between either the directionally decoupled or full spectral approach.

In this way, one can get an indication of the best modelling approach without having to implement and validate several individual wave models, and their tunings. Also, this focus on model assumptions may shed some light on the dominant physical processes in slanting fetch conditions and it may reveal deficiencies and sensitivities of parameterisations of physical processes. The latter will be done by investigating the effect of different formulations of the quadruplet source term in the SWAN wave model.

The contents of this paper are as follows. In Section 2 the area of interest and some experimental details will be discussed. Next, Sections 3 and 4 will present some numerical details, as well as a comparison between the numerical (SWAN) results and the present experimental data. In Section 5, the validity of the effective fetch concept will be investigated, whereas the role of the quadruplet interactions will be investigated in Section 6. Finally the conclusions and some considerations for future work will be presented in Section 7.

2. Area of interest and field data

The present area of interest is Lake IJssel in the Netherlands (Fig. 1), a lake of roughly 20 by 60 km. Up till 1932, Lake IJssel and Lake Marken used to be connected to the Waddenzee as they were part of the aforementioned 'Zuiderzee'. At present, they are large lakes with a typical depth of about 4–5 m; a significant part of their shores consists of dikes that were constructed between 1928 and 1976. Because many of these new shores are straight and artificial, it is potentially a highly suitable area for slanting fetch studies. This is all the more so because slanting fetch studies at sea tend to be hampered by significant amounts of swell (as in the study of Ardhuin et al., 2006) or tidal currents.

A disadvantage of Lake IJssel is that no well-aimed slanting fetch measurement campaign has taken place. Rather one has to rely on routine (non-directional) wave measurements that are carried out year-round by Rijkswaterstaat IJsselmeergebied (henceforth RWS IJG). The measurements mainly serve general investigations on wave climate and wave loading of dikes, as well as a number of aspects of wave model validation (Bottema et al., 2003). Considering the coastline and the position of the present measurement locations (Fig. 1), the location FL2 is best suited for the present analysis. FL2 is about 1.15 km from the eastern shore of Lake IJssel, which can be divided into two sections: a North–South shoreline section of 11.5 km length to the Southeast of FL2, and a SSW–NNE shoreline section to the Northeast of FL2, with a length of about 8.5 km.

Since 2000, capacitance wires are used for the wave measurements. In earlier years however, a step gauge with a resolution of 5 cm was used. The wind is measured at 10 m above the mean water level, using cup anemometers and wind vanes. The sample frequency is 4 Hz for the wave data and 1 Hz for the wind data. The wind data are stored as vectorial mean values of wind speed and wind direction, but in order to reduce scatter, hourly averages are used for the present analysis.

For the present study, seven years of data (1997–2004) are available in which the percentage of available data increased from order 50 to order 80%. A full description of the data set is described in Bottema (2007). Yearly averaged wind speeds and wave heights H_{m0} for the full data set are roughly 8 m s^{-1} and 0.4 m respectively. The severest conditions observed typically occurred during SW-winds of 21–24 m s^{-1} (9 Beaufort), with significant wave heights H_{m0} up to 1.4–1.8 m and peak periods T_p up to about 5.5 s. In De Waal (2001) and Bottema et al. (2003), further details are given about the data set, the validation of the SWAN wave model, and about the issue of depth-limited wave growth.

For the present analysis, all summer data (May–September) were excluded as a precaution. This was done because of the risk of marine growth. Such growth is difficult to detect from individual measurements but it may cause large errors, especially when the significant wave heights are of the order of 10–20 cm or less. Data were validated in three ways; first of all by screening the data for noise, suspect trends and outliers. Secondly, subsets of data for one location were inter-compared, including a check on the consistency of the capa-probe data with early step gauge data (Bottema, 2007). Finally, the results of different locations were checked for consistency, while taking into account any fetch and depth differences. After these validations, a few specific subsets of the remaining winter data were also excluded because of weather conditions (occasional frost and icing effects) or because of operational problems like temporary malfunctioning of electronic or communication components, or general instrument failure. Finally, we focussed on winds with an offshore (easterly) component and a wind speed range of 10–11 m/s. It would have been preferable to extend the range of non-dimensional fetches gxU_{10}^{-2} by using a wide range of wind speed classes, but we restricted our analysis to a single wind speed class for two reasons. The first reason is linked to the lack of strong easterly wind data, when the wind at FL2 is offshore. For wind speeds above 11 m/s too few data for a few wind directions would be available to obtain statistically reliable results. The second reason is linked to the fact that for wind speeds well below 10 m/s, the scatter in the data becomes too great. A significant part of the wave height scatter is probably due to atmospheric stability effects on the wind and wave growth. Young (1998) shows that large (10 °C) air–water

temperature differences significantly affect wave growth (11% effect on the wave height parameter H_{m0}, 21% on wave energy) up to wind speeds of 10 m s^{-1}. Inspection of satellite data and air temperatures of nearby land-based weather stations suggests that over Lake IJssel, 10 °C difference in air and water temperature is uncommon but not impossible. Hence, the present lower wind speed limit of 10 m s^{-1} seems to be justified by Young's (1998) result. Another error source is related to the fact that the peak period scatter during the weak winds discussed above may even become so large that T_p for the first kilometres of fetch (with H_{m0}-values of 0.2 m and less) becomes ill defined. In this case, the main cause is probably linked to non-local wave energy (swell-like conditions) and instationarity.

3. Numerical wave modelling

All model simulations were carried out with the SWAN wave model (Booij et al., 1999) in stationary mode. For the simulation of wave growth in slanting fetch, both a large computational domain (Fig. 1) and a fine resolution were needed. The large domain is needed because some wave components in slanting fetch conditions are actually propagating in an onshore direction. The fine resolution is needed because slanting fetch wave fields also contain short-fetch components. Recent studies of fetch-limited wave growth showed that SWAN needs as much as 15, 30 and 100 upwind grid points to make certain that discretisation errors at a given location are less than 10%, 5% and 2% respectively. The latter two options were far from feasible. Hence a domain size of 29 × 40 km was chosen, using a uniform grid with a spatial resolution of 80 m. This domain is adequate to simulate offshore winds at FL2, but for westerly (onshore) winds, a much larger domain would be required. With the fine resolution chosen, this was not feasible due to hardware limitations. In spectral space, we used 31 frequencies geometrically distributed between 0.08 and 1.9 Hz, and a directional resolution $\Delta\theta$ of 10°. Finer directional resolutions ($\Delta\theta = 5°$) were tested, but they led to less than 1% and 0.5° change in wave height and directional parameters. For the iteration process, a strict convergence criterion of 50 iterations was prescribed to make sure SWAN was well converged in all cases.

Except for the quadruplet interaction process, all physical model settings were in agreement with the default settings for SWAN, version 40.41. As for the quadruplet interactions, not only the default Discrete Interaction Approximation (DIA) was used, but also a slightly more accurate multiple-DIA technique (mDIA; Hashimoto and Kawaguchi, 2001) and an exact technique (Xnl; Van Vledder, 2006). The latter technique requires lots of CPU-time as – with other things being equal – Xnl requires over 300 times as much CPU as DIA. In addition some numerical settings were modified as Van Vledder (2006) recommends using a maximum frequency of at least 6 times the peak frequency if Xnl is used in SWAN. Hence, the present frequency domain was extended from 1.9 to 8 Hz (using 49 instead of 31 frequencies) while the number of iterations was increased to 70 to ensure full convergence. As the Xnl-approach in SWAN required about 300 times as much CPU time as DIA, Xnl could be used for one-dimensional (1D) sensitivity studies only. In those cases where Xnl was to be compared directly with DIA and mDIA (as in Section 6), the SWAN-simulations with DIA and mDIA were also run in one-dimensional mode. The general set-up of these 1D-studies was identical to the 2D simulations described above except for the absence of alongshore variations allowing to drop one spatial dimension. For all 1D simulations, the same computational domain was used; only the wind direction was varied from shore-normal (along the x-axis of the domain) to nearly shore-parallel. The length of the 1D computational domain was set at 24 km to make sure that even for nearly parallel fetch, the SWAN-1D results for the first kilometres off the coast would not be influenced by any potential disturbance originating from the end of the computational domain. As for the input parameters, a wind speed of 10.5 m s^{-1} was used, in accordance with the selected data subset with 10–11 m s^{-1} wind speeds. By lack of more detailed wind measurements or suitable wind model results, the wind speeds were assumed to be spatially uniform. Previous error estimates (Bottema et al., 2003) suggest that the use of uniform wind fields especially causes some H_{m0}-overestimation for fetches that are much smaller than the fetch of the wind reference location. For FL2, the use of uniform wind fields in cases with a wind blowing perpendicularly offshore might result in 20% nearshore overestimation of H_{m0} and about

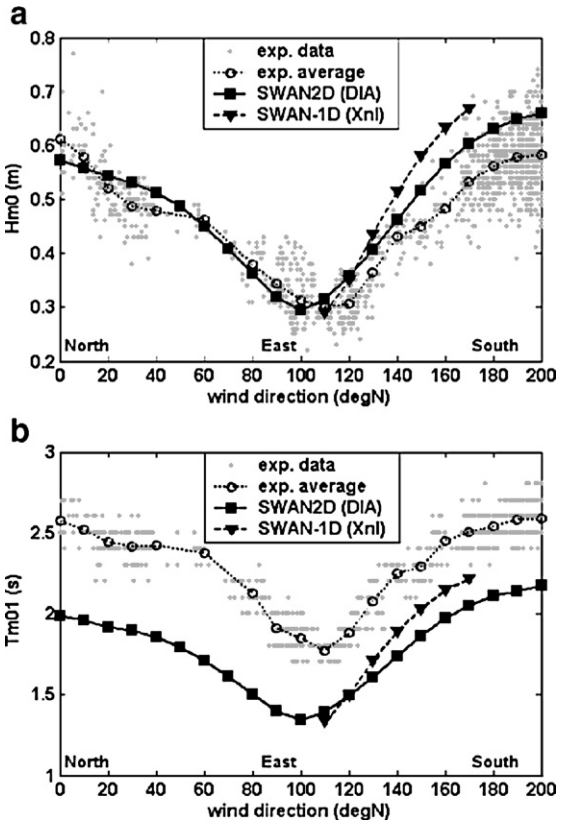

Fig. 2. Individual 20-minute samples (gray dots), averaged experimental data (open circles), SWAN-2D model results with DIA (black squares) and SWAN-1D model results with Xnl (closed triangles) for the measurement location FL2 and a wind speed of 10–11 m s^{-1}. (a) Wave height H_{m0} as a function of wind direction. (b) Wave period T_{m01} as a function of wind direction.

10% overestimation for most wave period measures. Additional analyses showed that the effects at the wind reference location itself (FL2) are order 5% on the wave height and order +3% on the wave periods. For slanting fetch, these effects are expected to be still smaller because of the increased fetch. In all cases, the cape-like shape of the coastline near FL2 probably mitigates the above effects. For the 2D simulations, we made use of the available lakebed grid of Rijkswaterstaat, which had a spatial resolution of 40 m. We also assumed a water level of 20 cm below the NAP datum, in accordance with the averaged experimental data. In the 1D simulations, a uniform water depth of 4.2 m was used corresponding to the average water depth over the first 15 km of the perpendicular fetch.

4. Measured and modelled wave parameters

Before discussing the tests on effective fetch and on quadruplet interactions, a general impression on the experimental and numerical data will be given. Fig. 2 shows the measured and simulated significant wave height H_{m0} and spectral period T_{m01} as a function of wind direction. It is clear that at the FL2-location, strongly sheltered conditions (with low and short waves) only occur for a wind nearly perpendicular to the coast (wind direction close to 90°). When the angle between the coast-normal and the wind increases, the wave heights (H_{m0}) also quickly increase. To a lesser extent, this also applies to the wave periods T_p, T_{m-10}, T_{m01} and T_{m02}. Because of the natural variability in the experimental data, not only individual 20-minute data are plotted, but also the averages for each 10° wind direction class. The relative uncertainty (one standard deviation divided by the mean) in these H_{m0}- and T_{m01}-averages is roughly 1.5%, while the relative scatter in the 20-minute values of H_{m0} and T_{m01} is typically about 8%.

For general validation results of the SWAN model with default settings, the reader is referred to Bottema et al. (2003). With southwesterly (onshore) winds, the wave height H_{m0} at FL2 and similar locations is generally adequately predicted, but T_p and T_{m01} are roughly 15% too low. This general picture of largely correct wave heights and underestimated wave periods also emerged from a range of other studies, for example Ris et al. (1999). As for the present SWAN results, Fig. 2 contains both results of the standard two-dimensional SWAN with DIA and SWAN-1D results with Xnl. For the latter, only the wind direction range of 110°–170° was considered, as this was the range with negligible differences between 1D and 2D simulations with SWAN-DIA; the differences were less than 3% for H_{m0} and T_{m01} and less than 1° for the directional spreading σ_θ and the mean wave direction θ. For directions smaller (more northeasterly) than 110° however, the kink in the coast line to the northeast of the FL2-location apparently had a non-negligible influence on the FL2 wave conditions. In all cases, SWAN tends to overestimate H_{m0} for slanting fetch (~140°) and especially parallel fetch (~180°); see Fig. 2a. In Fig. 2a, SWAN with DIA-quadruplets fits better with the measurements than SWAN with Xnl, especially for slanting and nearly parallel fetch. A small part of this effect may be caused by the fact that with Xnl, SWAN was run in 1D mode, which tends to overestimate wave energy in along shore directions by up to a few percent. The results for the wave period T_{m01} are shown in Fig. 2b. With DIA-quadruplets, SWAN underestimates the measured T_{m01} by about 25% for all wind directions. With Xnl, SWAN does a slightly better job, especially for nearly parallel fetch where the T_{m01}-underestimation is reduced to about 10%.

For a number of stationary data with H_{m0}-values representative of the means plotted in Fig. 2a, wave spectra were analysed as well. In the spectral tail, SWAN-DIA and SWAN-Xnl produced very similar results (Fig. 3). Both overestimated wave energy while the slope of the tail was slightly underestimated. Near and below the spectral peak, SWAN with Xnl has a significantly more peaked spectrum than SWAN-DIA. For these lower frequencies, the measurements do not immediately show a clear preference for the spectral shape as predicted by either SWAN-DIA or SWAN-Xnl. However, close inspection suggests that like the advanced SWAN-Xnl, the experimental spectra are somewhat more peaked than the standard SWAN-DIA spectra.

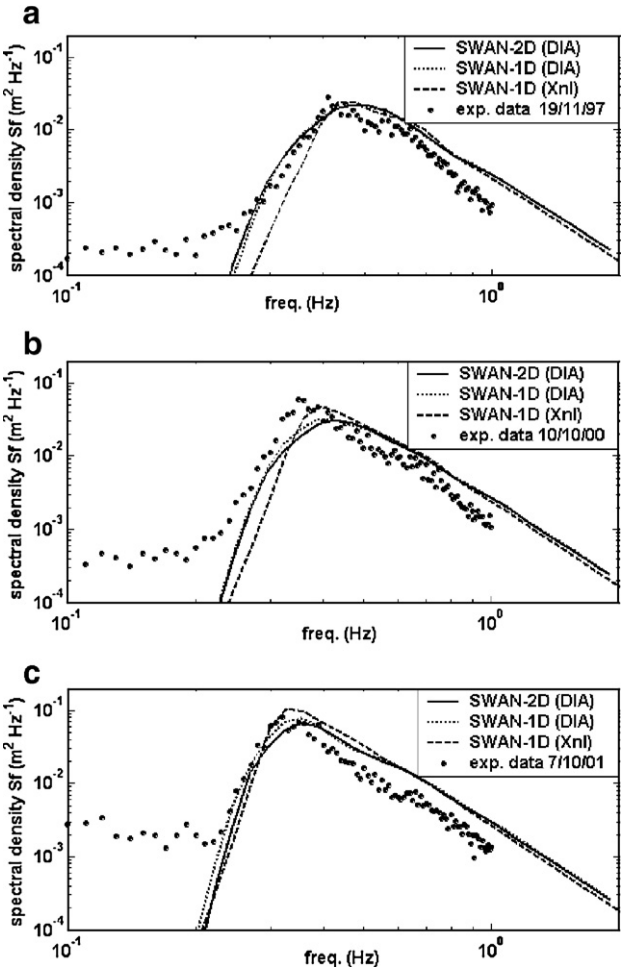

Fig. 3. Wave spectra for South-Easterly wind (10.5 m s^{-1}; 120–150°). The SWAN-2D results with DIA and the SWAN-1D results with DIA and Xnl are plotted as thick solid dotted and dashed lines respectively. Experimental data are plotted as small circles (a) Wind direction 120°, 19 Nov. 1997, 10–11 h MET (b) Wind direction 130°, 10 Oct. 2000, 3–4 h MET (c) Wind direction 150°, 7 Oct. 2001, 22–23 h MET.

5. Validity of the effective fetch concept

Simple wave growth formulas like for example those of Bretschneider (CERC, 1984), Kahma and Calkoen (1992) and Young and Verhagen (1996) generally rely on the use of an effective fetch to model the wave conditions in practical situations. In the present section, the validity of the effective fetch concept will be investigated using three different approaches:

- inspection of the wave steepness data (the relevance of this parameter will be discussed below).
- describing the present measurements of wind, wave heights and wave periods in terms of an effective fetch for the latter two parameters, and comparing those fetch values.
- describing the SWAN wave heights and wave periods in terms of an effective fetch by comparing the SWAN results in slanting fetch with the SWAN results in a 1D-situation with wind blowing perpendicularly off a coast.

The latter case with SWAN results has the advantage of a self-consistent data set without experimental errors, as one no longer needs to combine measurements with a given empirically-based parametric wave growth curve. On the other hand, one should be strongly aware that SWAN is only an approximation to reality. Finally, it is noted that only wave heights and wave periods are considered in this section; the wave directions and directional spreading will be discussed in Section 6.

5.1. Verification of effective fetch concept with wave steepness data

For wind sea, the wave heights, wave periods and wave lengths are much more sensitive to fetch and wind speed variations than the wave steepness, since the fetch- and wind-related wave height and wave length trends tend to partly cancel out each other. This suggests that a comparison between measured steepness data in complex situations and predicted steepness data from a wave growth formula might give clues about the (local) validity of the effective fetch concept. As most wave growth formulas are far too complex to allow for an easy calculation of the wave steepness, we focussed on the work of Kahma and Calkoen (1992). At the end of their paper, they give some simple formulas to fit the dimensionless wave energy and dimensionless peak frequency of their composite data set. These can be converted to the following formulas for H_{m0} and T_p:

$$H_{m0} = 4\sqrt{5.2\times10^{-7}}\frac{U_{10}^2}{g}\left(\frac{gx}{U_{10}^2}\right)^{0.47} \quad (1)$$

$$T_p = \frac{2\pi}{13.7}\frac{U_{10}}{g}\left(\frac{gx}{U_{10}^2}\right)^{0.27} \quad (2)$$

where U_{10} is the wind speed at 10 m height, g the gravitational acceleration (9.81 m s^{-2}) and x the fetch (m). Note that both formulas are valid in the deep water approximation only. The next step is to combine Eqs. (1) and (2) into a deep water steepness $s=H_{m0}/L(T_p)=2\pi H_{m0}/(gT_p^2)$, yielding

$$s \approx 0.086\left(\frac{gx}{U_{10}^2}\right)^{-0.07} \quad (3)$$

Eq. (3) shows that the relation between wave steepness, wind speed and fetch is weak indeed. For the present case, typical ranges for x and U_{10} are 1–30 km and 10–11 m s^{-1} respectively. This yields wave steepness values in the range of $0.049<s<0.062$, where the largest steepness occurs for the shortest fetch. No such simple T_p based steepness expressions exist for the Bretschneider formulas of (CERC, 1984), which are to be presented in Section 5.2 The Bretschneider steepness has the same decreasing trend with fetch, but the values are slightly lower. For the above fetch range and a 10.5 m s^{-1} wind speed, the Bretschneider steepness ranges from 0.040 to 0.061 in deep water, and 0.043 and 0.063 when the water depth is 4.2 m, like in Lake IJssel.

Fig. 4 shows that many of the FL2 measurement data are outside the theoretical steepness range mentioned above; the differences are clearly large enough to exclude any effect of random errors. Systematic experimental errors in T_p are unlikely anyway. For H_{m0}, drift and slight non-linearities in the capa-probe response are potential error sources. However, errors greater than 5% are unlikely as for given wind conditions and sufficient sample sizes (at least 50), the relative H_{m0} difference between the present step gauge and capa-probe data subsets was always less than +/−5%.

All in all, Fig. 4 gives clear indications that the real steepnesses are lower than predicted by Eq. (3) during slanting and parallel fetch. This is in line with the results of Pettersson (2004), who found for wind blowing obliquely off a coast, the dimensionless wave energy for a given dimensionless wave frequency (and independent of the fetch definition) was roughly 50% lower than expected from Kahma and Calkoen (1992). It is important to note that SWAN-simulations for the present case suggest that noticeable bottom friction effects already occur for wave heights of 0.5 m. In Fig. 4, this corresponds to wave directions of 20° and less, or 160° and more. Hence, no definitive conclusions can yet be drawn for the parallel fetch case.

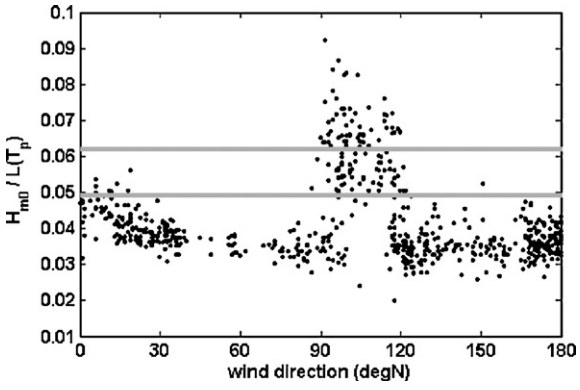

Fig. 4. Measured wave steepness $H_{m0}/L(T_p)$ as a function of wind direction for the location FL2 and for a wind speed of 10–11 m/s. Each dot represents a 20-minute data point. Thick lines represent the theoretical range from Eq. (3); the upper and lower line correspond to 1 and 30 km of fetch respectively.

For the slanting fetch case however, there are now some first indications that at the location FL2, and during offshore winds, the effective fetch concept may not be valid.

A final feature worth noting in Fig. 4 is related to the elevated steepnesses for wind directions between 90° and 120° (E-ESE winds). It is not yet clear whether the elevated steepness is related to the short fetch for these wind directions, or to the effect of the kink in the coastline.

5.2. Verification of effective fetch with inverse wave growth formulas

The above wave steepness analysis is instructive but sensitive to errors. In our case, a power mismatch in Eq. (3) of only 0.01 yields already 8% wave steepness error. For the present analysis, we chose an 'inverse wave growth formula' approach. Rather than calculating a wave height and wave period from a given fetch and wind speed, we did the opposite and calculated the effective fetch from the measured wind and wave conditions. By comparing the 'wave-height-fetch' x_H and 'wave-period-fetch' x_T it is then possible to quantify deviations from the effective fetch concept. By using such an inverse approach, we do not need to select any particular method for calculating effective fetches, and thereby, we avoid making any a-priori assumptions about the directional wave energy distribution. The concept of inversed wave growth formulas was introduced by Donelan et al. (1992) to derive deep water growth curves using an incremental growth analysis. Young (1997) extended this method to shallow water growth curves. In our study, however, inverse relations were applied to the full fetch to determine fetch lengths as a function of wave parameters at a specific location.

For the wave growth formulas of Kahma and Calkoen (1992), the evaluation of x_H and x_T is fairly straightforward as the expressions for these parameters can easily be derived from Eqs. (1) and (2):

$$x_H = \frac{U_{10}^2}{g}\left(\frac{1}{4\sqrt{5.2\times10^{-7}}}\frac{gH_{m0}}{U_{10}^2}\right)^{\frac{1}{0.47}} \approx 253585\cdot g^{1.13}U_{10}^{-2.26}H_{m0}^{2.12} \tag{4}$$

$$x_T = \frac{U_{10}^2}{g}\left(\frac{13.7}{2\pi}\frac{gT_p}{U_{10}}\right)^{\frac{1}{0.27}} \approx 17.94\cdot g^{2.70}U_{10}^{-1.70}T_p^{3.70} \tag{5}$$

However, the above formulas are only valid for deep water. Furthermore, previous research has shown that it may be difficult to fit different data sets to a single wave growth curve (Kahma and Calkoen, 1992). For that reason, other wave growth formulas were chosen as well. For practical reasons, we looked for formulas for H_{m0} (or wave energy E) and T_p with scaling on the U_{10} wind speed, which were applicable for both deep and intermediate water. This resulted in adding the Lake George formulas of Young and Verhagen (1996) and the well-known Bretschneider formulas (CERC, 1984) to our analysis. These formulas were too complex to express them in terms of an effective fetch so we present them in their usual form. The Young and Verhagen (1996) formulas for the wave energy read:

$$\varepsilon = \frac{1}{16}\left(\frac{gH_{m0}}{U_{10}^2}\right)^2 = C_1\left[\left[\tanh\left(A_1\right)\right]\tanh\left(\frac{B_1}{\tanh\left(A_1\right)}\right)\right]^{p_1} \tag{6}$$

where $C_1=3.64\times10^{-3}$, $p_1=1.74$ and:

$$A_1 = 0.493\delta^{0.75} = 0.493\left(\frac{gd}{U_{10}^2}\right)^{0.75} \tag{7}$$

$$B_1 = 3.13\times10^{-3}\chi^{0.57} = 3.13\times10^{-3}\left(\frac{gx}{U_{10}^2}\right)^{0.57} \tag{8}$$

while the Young and Verhagen (1996) formulas for the wave frequency are:

$$\nu = \frac{U_{10}}{gT_p} = C_2\left[\left[\tanh\left(A_2\right)\right]\tanh\left(\frac{B_2}{\tanh\left(A_2\right)}\right)\right]^{p_2} \tag{9}$$

where $C_2=0.133$, $p_2=-0.37$ and:

$$A_2 = 0.331\delta^{1.01} = 0.331\left(\frac{gd}{U_{10}^2}\right)^{1.01} \tag{10}$$

$$B_1 = 5.215\times10^{-4}\chi^{0.73} = 5.215\times10^{-4}\left(\frac{gx}{U_{10}^2}\right)^{0.73} \tag{11}$$

The Bretschneider formulas (CERC, 1984; Young and Verhagen, 1996) have largely the same form, but different constants, parameters and powers. For the wave heights and wave energies, these are: $C_1=5\times10^{-3}$, $p_1=2$, $A_1=0.53\delta^{0.75}$ and $B_1=5.65\times10^{-3}\,\chi^{0.5}$. For the wave periods, the Bretschneider parameters are: $C_2=0.133$, $p_2=-1$, $A_2=0.833\delta^{0.375}$ and $B_2=3.79\times10^{-2}\,\chi^{0.33}$.

The results for all the above-mentioned wave growth formulas are presented in Fig. 5. Fig. 5a shows the fetch that would yield the same H_{m0} and T_p as at the FL2 measurement location, using the Kahma–Calkoen-derived relations (4) and (5), and using the measured wind speed and water depth (about 10.5 m s^{-1} and 4.2 m respectively). Only results for wind directions in the range of 20° to 160° are shown, as some bottom friction effects may occur for the remaining wind directions (see the previous sub-section). Inspection of Fig. 5a shows that the wave height and wave period fetches x_H and x_T differ by more than a factor 2 for most wind directions, especially during slanting or parallel fetch. This corresponds to differences in either H_{m0} or T_p of 40% and 20% respectively (assuming $H_{m0}\sim x^{0.47}$ and $T_p\sim x^{0.27}$). The only situation where the difference between x_H and x_T is relatively small (<40%) occurs for wind directions of 90°–110° (Fig. 5a) when the winds are close to shore-normal.

It should be noted that the above differences in fetch, as derived from H_{m0} and T_p, are much larger than the effect of any of

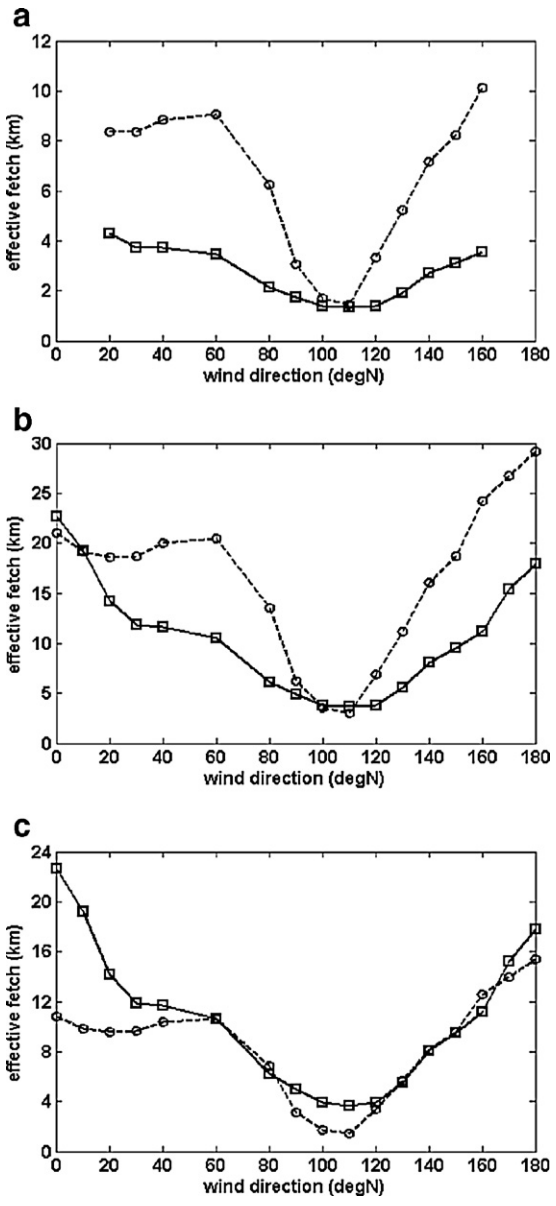

Fig. 5. Effective wave height fetch (square points, solid line) and peak period fetch (open circles, dashed line) that would yield the same H_{m0} and T_p as measured at the FL2-location if the wind speed and water depth are about 10.5 m s^{-1} and 4.2 m respectively. The upper, middle and lower plots correspond to estimates according to (a) Kahma and Calkoen (1992), (b) Bretschneider (CERC, 1984) and (c) Young and Verhagen (1996) respectively.

the assumptions and experimental errors. This certainly applies for the peak period T_p (<3% error, random only). In H_{m0}, biases of 5–10% are possible but unlikely (see previous sub-section) so that even the largest error source cannot explain the above fetch difference in x_H and x_T, which is equivalent to 40% H_{m0} difference. As for the wind speed errors, 10% error is expected to cause about 23% fetch error in x_H and 17% in x_T, see Eqs. (5) and (6). As a result, these errors will mainly affect the absolute fetches, while the effect on the x_H/x_T ratio is rather small. Summarizing, errors (biases) in the measured wind speed are unlikely to exceed 2% so the main error source (order 5% error) is related to the lack of complete wind field data, which leads to the unavoidable assumption of a spatially uniform wind (Section 3).

With the Bretschneider curves (CERC, 1984), the calculated fetches (Fig. 5b) are typically 2.2 to 3 times larger (for T_p and H_{m0} respectively), but otherwise the trends are quite similar to the results for the Kahma and Calkoen (1992) formulas. Again, the wave period fetch x_T during slanting fetch conditions is often about twice as large as the wave height fetch x_H whereas x_T and x_H differ only very little for nearly shore-normal winds with directions of 90°–110°. Remarkably, x_T is also significantly higher than x_H for onshore winds (not shown in the plot), which implies that the Bretschneider wave steepnesses are lower than the observed ones. The fetch x_T for onshore winds is about 37 km whereas x_H then roughly is 27 km. Especially the calculated x_T-fetch appears to be rather large as the actual distance between FL2 and the South-Westerly shores of Lake IJssel is of the order of 20 km.

The results for the Young and Verhagen (1996) formulas (Eqs. (6)–(11)) are shown in Fig. 5c. Their x_H is nearly identical to the Bretschneider x_H in Fig. 5b. Their x_T is smaller than the Bretschneider x_T in Fig. 5b, but it is quite close to the Kahma–Calkoen value in Fig. 5a. Remarkably, the x_T and x_H of Young and Verhagen agree best with each other in conditions with slanting or near-parallel fetch (about 70° and 150°) while the x_H and x_T of Kahma–Calkoen and Bretschneider seem to agree best for shore-normal winds. These results seem to suggest that the Young and Verhagen (1996) growth curves may be inadvertently tuned to the special case of slanting and (nearly) parallel fetch. Actually, such a 'tuning' could well have occurred because of the slightly elongated shape of Lake George, and because the data selection of Young and Verhagen (1996) focussed on winds along the long axis of the lake.

All in all, the following can be concluded from this section:

- For most wind directions, our measured H_{m0} and T_p cannot be accurately predicted by either of the tested wave growth formulas, unless different effective fetches are assigned to H_{m0} and T_p.
- Comparison of Fig. 5a, b and c shows that different wave growth formulas yield considerable differences in x_H and x_T, or in H_{m0} and T_p if they are used in the conventional way. Ris et al. (2001) also found similar large differences The present results suggest that differences in wave growth formulas are not only caused by atmospheric conditions (as suggested by Kahma and Calkoen, 1992) but also by the fetch geometry of the underlying data, so that the optimum formula for a given case also depends on the fetch geometry under consideration.

5.3. Verifying the effective fetch hypothesis with SWAN

Verifying the hypothesis of effective fetch with a combination of measurements and simple wave growth formulas is far from trivial, as is shown in the previous sub-section. In the present sub-section, the effective fetch hypothesis will be verified with SWAN model results. Although there are certainly differences between SWAN and reality (see Figs. 2 and 3), this SWAN model approach still has four major advantages. Firstly, the effective fetch hypothesis can be investigated for several locations, instead of just one. Secondly, the effective fetches can be considered for several types of wave period measures, instead of just one. Thirdly, the effects of various modelling techniques affecting the directional coupling can be

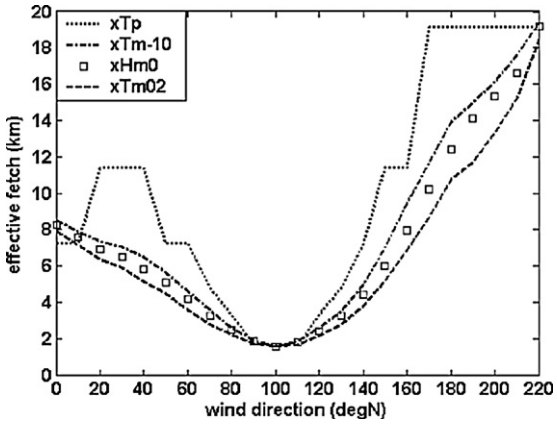

Fig. 6. Fetch values x_{T_p} (dotted line), $x_{T_{m\text{-}10}}$ (dash–dot line), $x_{H_{m0}}$ (square points) and $x_{T_{m02}}$ (dashed line) in a SWAN-1D simulation with shore-normal wind that yield the same T_p, H_{m0}, $T_{m\text{-}10}$ and T_{m02} for the FL2-location as in a SWAN-2D simulation with the same input and numerical settings. The results are plotted as a function of wind direction.

investigated. This approach is explored in Section 6 of this paper. Finally, this approach allows one to verify the effective fetch hypothesis for a consistent set of data and without the interference of various assumptions. This in contrast with the previous analysis, which assumes a uniform wind field and, more importantly, relies on the assumption that the present experimental data can be well described by the wave growth formulas under consideration. The large differences between Fig. 5a, b and c suggest that the latter assumption does not necessarily hold.

The effective fetches in the present SWAN analysis are not calculated from the coast-line geometry but by comparing the actual SWAN based wave height and wave period to a SWAN-benchmark simulation. This benchmark simulation was a 1D SWAN-calculation with shore-normal wind direction, and the same numerical settings, wind speed and bottom depth as in the actual simulations. For the latter simulations, we stored the H_{m0} for each point of interest, and we linked these H_{m0}-values to the shore-normal distance to the coast in the 1D benchmark simulation. In this way, we obtained SWAN-estimates for the fetches $x_{H_{m0}}$, x_{T_p}, $x_{T_{m\text{-}10}}$, $x_{T_{m01}}$ and $x_{T_{m02}}$, related to the wave height H_{m0} and the wave period measures T_p, $T_{m\text{-}10}$, T_{m01} and T_{m02} respectively.

In Fig. 6, the effective fetches for the FL2-location are plotted as a function of wind direction; the underlying wave heights and wave periods were already shown in Fig. 2. Fig. 6 shows that $x_{H_{m0}}$ and x_{T_p} only agree well for wind directions of 90°–110° (nearly shore-normal winds). For other wind directions and especially for slanting and parallel fetch, the peak period fetch x_{T_p} is up to a factor 2 larger than the wave height fetch $x_{H_{m0}}$. These trends are highly similar to the general trends of Fig. 5a and b, where the fetches were calculated from the present measurements and the Kahma and Calkoen (1992) and Bretschneider (CERC, 1984) formulas. The absolute values of the SWAN fetches tend to fall somewhere between the (greatly differing) Kahma–Calkoen and Bretschneider fetches. Another main feature of Fig. 6 is the fact that the wave period fetches $x_{T_{m\text{-}10}}$, $x_{T_{m02}}$ and especially $x_{T_{m01}}$ (not shown) are much closer to the wave height fetch than the peak period fetch x_{T_p} that has been considered so far. This would imply that – at least for the present wave growth stage – the validity of the effective fetch hypothesis strongly depends on the wave period measure under consideration. A further point of interest is that in slanting and parallel fetch conditions, the $x_{T_{m\text{-}10}}$ fetch is systematically larger than the $x_{T_{m02}}$ fetch. As $T_{m\text{-}10}$ is far more sensitive to low-frequency contributions than T_{m02}, this may be an indication that in those conditions, there is a relatively large contribution of long fetch and on-shore wave components (or a small contribution of short-fetch and high-frequency components) in the wave field. Apparently, this seems to be even more true for the peak period T_p and its fetch x_{T_p}. In fact, x_{T_p} during slanting fetch can be twice as large as the other wave period measures. At first sight, this difference seems extremely large. However, in terms of the wave period ratios $T_{m\text{-}10}/T_p$, T_{m01}/T_p and T_{m02}/T_p, the difference is not more than about 20%. A final point of interest is the step-like behaviour of the peak period fetch x_{T_p}. This step-like behaviour is caused by the fact that the SWAN wave frequencies each are 10% apart (as recommended by the manual), which implies that all realisable SWAN peak periods are also 10% apart. It is noted that a recent version of SWAN, version 40.51, uses a parabolic fit to obtain smoother estimates of the peak frequency. However, it is not expected that this fit will change the outcomes of this study, even though this fit is doubtlessly a useful improvement to SWAN.

In Fig. 7, the effective SWAN fetches are plotted as a function of distance to the coast along an East–West transect through the measurement location FL2. Fig. 7a gives the results

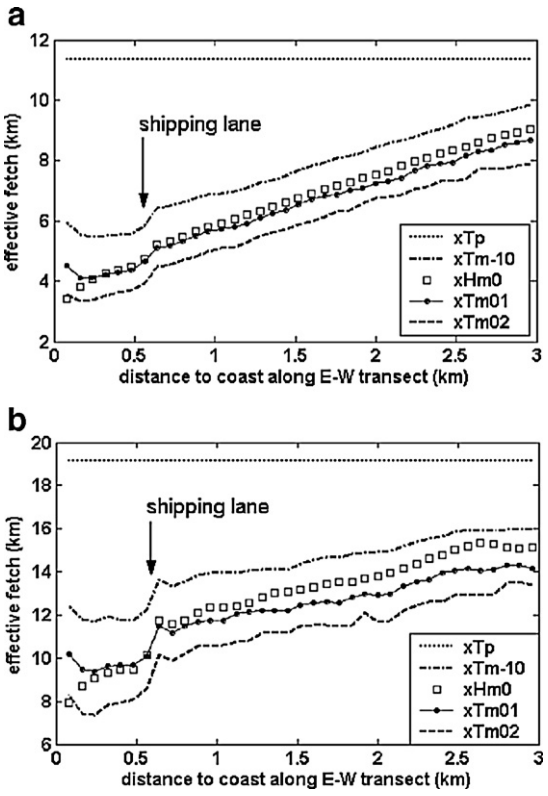

Fig. 7. Fetch values x_{T_p} (dotted line), $x_{T_{m\text{-}10}}$ (dash–dot line), $x_{H_{m0}}$ (square points), $x_{T_{m01}}$ (thin solid line with circles) and $x_{T_{m02}}$ (dashed line) in a SWAN-1D simulation with shore-normal wind that yield the same T_p, H_{m0}, $T_{m\text{-}10}$, T_{m01} and T_{m02} as in a SWAN-2D simulation with the same input and numerical settings. The results are plotted as a function of distance to the coast as measured along a shore-normal axis (East–West) through the FL2-location, both for wind directions of 150° (a) and 180° (b).

for slanting fetch (wind direction SSE/150°); Fig. 7b gives the results for parallel fetch (S/180°). In both cases, the (fetches for the) peak periods in the first 3 km off the coast are constant. Notice that both the peak period and the other wave periods yield non-zero fetch values very close to the coast. Finally, the small kink at about 700 m off the coast is caused by a shipping lane at 700 m off the shore (See Fig. 1). This interrupts the otherwise flat bottom and yields a slight and localised wave height and wave period increase.

Fig. 7 also shows that in slanting and parallel fetch conditions, the effective fetch concept clearly does not hold for the peak period T_p. Very close to the coast, x_{T_p} is roughly 2.7 times as large as x_H. Three kilometres off the coast, the difference is still a factor 1.27. These differences in $x_{H_{m0}}$ and x_{T_p} would correspond to a H_{m0}-mismatch of 60% and 12% respectively, or a T_p-mismatch of 31% and 7%. For the fetches $x_{T_{m-10}}$ and $x_{T_{m02}}$, the absolute difference with the fetch $x_{H_{m0}}$ is roughly constant along the transect. The relative differences between $x_{T_{m-10}}$ and $x_{H_{m0}}$ decrease from 65% at the shore to 9% at 3 km offshore. Using $x_{T_{m-10}}$ to predict H_{m0} then results in a H_{m0}-mismatch of the order of 27% and 4% respectively. For the $x_{T_{m02}}$-fetch, the results are largely comparable. For $x_{T_{m01}}$-fetch, the mismatches are somewhat smaller in the parallel fetch case and clearly smaller in the slanting fetch case.

All in all, the present results suggest that the validity of the effective fetch concept strongly depends on the wave period parameter that is used in conjunction with it. With the mean period T_{m01} (or with T_{m-10} or T_{m02}), the effective fetch concept performs much better than with the peak period T_p. If during slanting and parallel conditions, the effective fetch concept is used too close to the coast, the difference between the wave height fetch x_H and some of the wave period fetches x_T may be well above 20% (see Fig. 7 and the above discussion), resulting in a potential H_{m0}-mismatch of 10% and more. For that reason, one should preferably not rely on the effective fetch concept in the first 1–3 km off the coast. The latter distance of 3 km applies for joint parametric predictions of H_{m0} and T_p. With other spectral wave period measures (such as T_{m-10}, T_{m01}, T_{m02}), a minimum shore-normal distance of up to 1 km is typically sufficient to safely apply the effective fetch concept.

6. Role of the quadruplet interactions during slanting fetch

In the present section, the role of the non-linear four-wave (quadruplet) interactions will be investigated, assuming that a directionally decoupled approach is only valid if the effect of the quadruplet interactions on the wave parameters is negligible. Quantifying the effect of the quadruplets is no easy task because no model is known where the quadruplets can be activated and de-activated without affecting the whole source term balance. Hence, we investigated the role of the quadruplets by leaving them activated, but by considering three different quadruplet formulations in SWAN: the DIA, mDIA and Xnl approaches presented in Section 3. Any significant difference in more complex situations might be attributed to the effect of the different quadruplet formulations as in a 1D fetch-limited wave-growth situation, each quadruplet approach yields virtually identical wave growth in terms of H_{m0} and T_{m01}.

To investigate the role of the quadruplet interactions SWAN 1D computations were made. These computations revealed that only for very short fetches (<1 km), the mDIA and Xnl results differed from the DIA results by more than 2% (for T_{m01}) to 3% (for H_{m0}).

Fig. 8a shows the wave height as a function of wind direction, for a fetch that is typical of the FL2-location. Wind directions of 90° and 180° correspond to perpendicular and parallel fetch respectively, and to easterly and southerly winds in reality. In comparison to DIA, mDIA yields up to 3% H_{m0}-reduction for wind directions that are slightly off coast-normal and up to 3% H_{m0}-increase for nearly parallel fetch. Similar trends were observed for various wave period measures — Fig. 8b shows the results for T_{m01}. The Xnl-simulations show trends similar to mDIA, but the differences with DIA are up to 6%. Remarkably, the lowest H_{m0} in the Xnl-simulations did not occur for perpendicular fetch but for a 100° wind. This seems to be due to some spurious low-frequency energy (as will be shown in Fig. 10) at short fetches for the case of 90° winds.

In slanting and parallel fetch conditions, the mean wave direction θ may deviate considerably from the wind direction, a phenomenon that is not captured by the simple wave growth formulas in Section 5. The deviations are such that the wave directions appear to be 'steered' by the coastline. This 'wave steering' $\Delta\theta$ (Fig. 9a) was investigated for three different wind speeds (8, 10.5 and 13 m s^{-1}) but no dependence of the wave

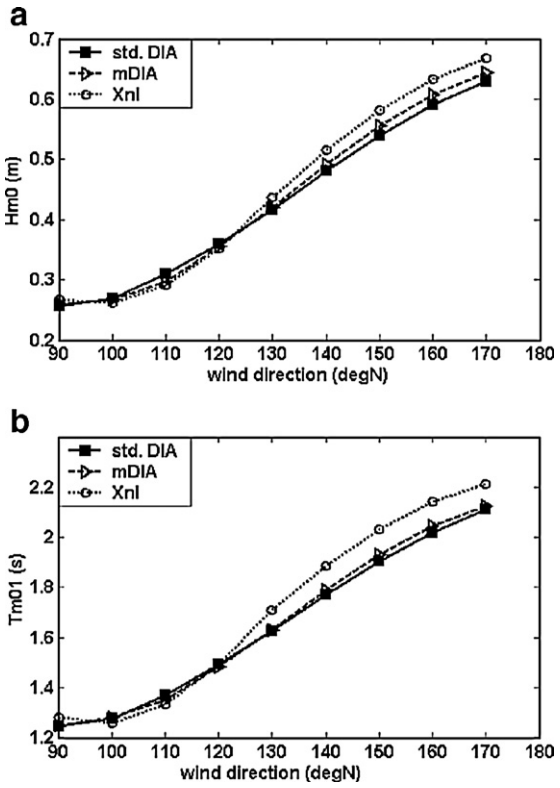

Fig. 8. Wave height H_{m0} (a) and mean wave period T_{m01} (b) from SWAN-1D as a function of wind direction (orthogonal fetch x=1120 m), where 90° is shore-normal wind and 180° wind parallel to the shore (to be compared with easterly and southerly wind in reality). Results with DIA, mDIA and Xnl-quadruplets are indicated with squares, triangles and circles respectively.

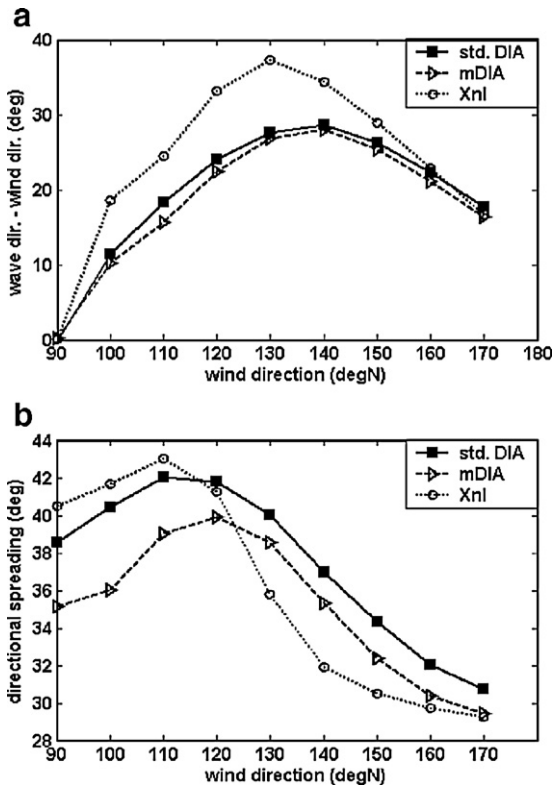

Fig. 9. SWAN difference between wind and wave direction (a) and SWAN directional spreading (b) as function of wind direction. Fetch and notation as in Fig. 8.

steering on the wind speed was found. This suggests that the wave steering does not scale with the dimensionless fetch (gx) U_{10}^{-2}. Rather, a strong dependence on the orthogonal fetch x_N (along the shore-normal) itself was found: for 0.8 km $< x_N <$ 5 km, the wave steering was approximately proportional to $x_N^{-0.5}$. The wave steering parameter $\Delta\theta$ also seems to be relatively sensitive to the effect of the quadruplet interactions. The maximum amount of wave steering in Fig. 9a is about 28° for DIA but as much as 36° for Xnl. This maximum occurs when the angle between the wind and the coastline is about 45°. For nearly parallel fetches, the differences between DIA and Xnl become small. Still, the amount of wave steering is significant enough (17°) to result in a wave direction that is (slightly) onshore while the wind direction is (slightly) offshore. All in all, the following approximate but convenient parameterisation for the amount of wave steering $\Delta\theta$ at distances of 0.8 to 5 km from the coast is proposed for a first guess of the local wave direction (to be used if no model results are yet available):

$$\Delta\theta = \Delta\theta_{\max} \sin\left(\frac{9}{5}\times 2\pi\phi\right)\left(\frac{x_N}{1120}\right)^{0.5} \qquad (12)$$

where ϕ is the angle between the coast-normal and the wind, and $\Delta\theta_{\max}$ the maximum amount of wave steering in Fig. 9a (28° for DIA, 37° for Xnl).

Compared to perpendicular fetch, the directional spreading σ_θ initially tends to increase from normal to slanting fetch, and to decrease from slanting to parallel fetch (Fig. 9b). These trends appear to be strongest for fetches of the order of 1 km. A comparison of the different quadruplet formulations shows that σ_θ for mDIA is about 4° lower than the other formulations for winds that are close to shore-normal, whereas Xnl is about 3° lower for slanting fetch conditions. The explanation of these trends is far from trivial as the trends in σ_θ are reflected in none of the other integral wave parameters. There is little experimental evidence to verify the above σ_θ-trends, but Pettersson (2004) reports 10° σ_θ-decrease for slanting and narrow fetch. The latter is confirmed in our computational data, assuming that narrow and parallel fetch are largely comparable cases. For slanting fetch, the agreement is not so clear as our results suggest that (the reduction in) σ_θ strongly depends on the degree of slanting fetch. For strongly slanting fetch (160°), we found σ_θ-reductions of 6° (DIA, mDIA) to 10° (Xnl); see Fig. 8b. For slightly slanting fetch (110°–120°) however, we found no decrease but an increase in σ_θ of about 3°. All in all, the Xnl-trends for σ_θ (Fig. 9b) seem to be much closer to Pettersson's (2004) observational trends than the trends for DIA or mDIA. Fig. 10 shows some variance spectra for perpendicular and slanting fetch (90° and 130°). Only the results with DIA- and Xnl-quadruplets are shown as the differences between the DIA- and mDIA-results are relatively small. Overall, the DIA and Xnl-spectra look quite similar, although the Xnl spectra are somewhat more peaked. However, the Xnl-spectrum for perpendicular fetch (90°) shows a small hump at about 0.4 Hz. The hump occurs for all fetches of about 1 km and less, and in absolute terms, it remains almost constant. In relative terms, its relevance is largest for very short fetches (the first grid points off the coast). The aforementioned hump probably must be considered as spurious, since for simple 1D wave growth without swell, none of the current spectral shapes (such as JONSWAP, TMA, etc.) include any humps or secondary maxima below the peak frequency.

A remarkable result of both the DIA- and Xnl-simulations is the fact that slanting fetch conditions can be recognised by the shape of the one-dimensional wave spectrum, especially by the normalised height of the spectral peak, $\max(S_f)/(H_{m0}^2 T_p)$. With DIA $\max(S_f)/(H_{m0}^2 T_p)$ tends to be about 0.15 for perpendicular fetch, and about 0.07 for slanting fetch, the latter being an indication of a relatively flat spectral peak. With Xnl, both peak values are roughly a factor 1.5 higher than with DIA. The experimental data of Pettersson (2004) for inverse wave ages $U_{10}/c_p < 2$, where c_p is the phase speed of the waves, also show relatively flat spectral peaks for slanting (and narrow) fetch. In

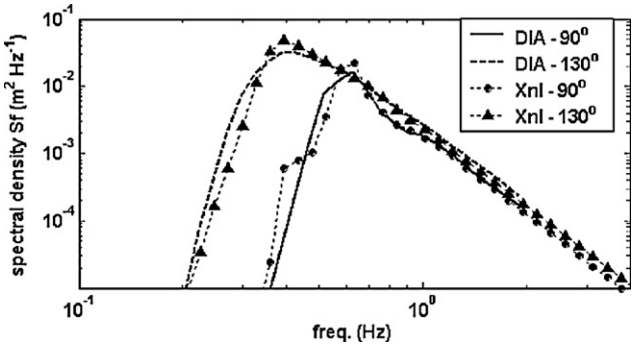

Fig. 10. SWAN variance spectra (log–log scale) with DIA- and Xnl-quadruplets, for a shore-normal distance of 1120 m, for perpendicular fetch (90°) and for slanting fetch (130°).

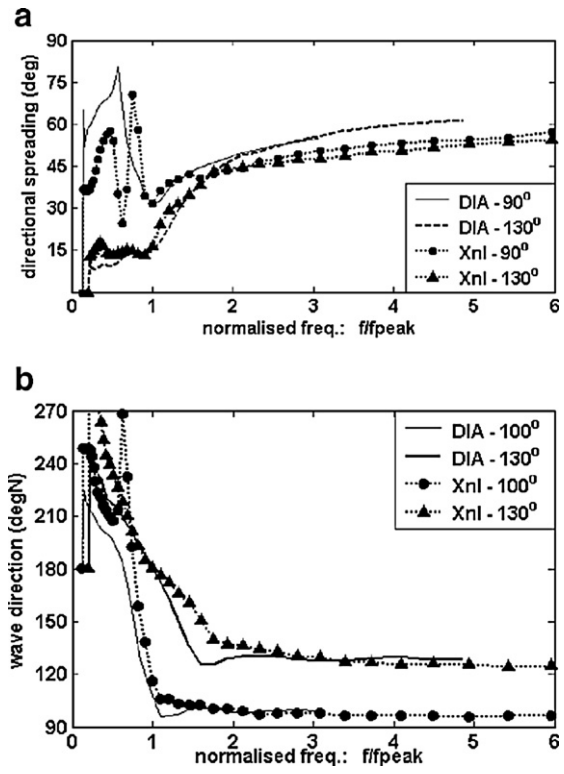

Fig. 11. SWAN directional spreading (a) and SWAN mean wave direction (b) as a function of normalised frequency f/f_p, for the same cases as in Fig. 10, except for Fig. 11b where slanting fetch (130°) is compared with near-perpendicular fetch (100°).

the present slanting fetch case (Fig. 10), U_{10}/c_p, with c_p based on T_p, is about 4. This suggests that for a sufficiently straight coastline, the above effects can also be observed for rather young waves.

Fig. 11a shows the spectral directional spreading $\sigma_\theta(f)$ as a function of f/f_p where f is the frequency and f_p the peak frequency. The differences between perpendicular and slanting fetch mainly occur near and below the peak frequency, where the directional spreading for slanting fetch is about 15° only. This is 2–5 times lower than for perpendicular fetch. In the high-frequency tail, locally generated waves dominate, and the fetch conditions have little or no effect. For all frequencies, there are clear differences between the DIA- and Xnl-approach. The irregular low-frequency behaviour of Xnl at perpendicular fetch is probably due to the spurious spectral hump mentioned before. Elsewhere, Xnl yields slightly larger $\sigma_\theta(f)$-values just above the spectral peak, but roughly 5° lower values in the spectral tail. The Xnl trends for $f/f_p>1$ (and $\sigma_\theta(f)$) agree excellently with Pettersson's (2004) data for both normal and slanting fetch. For DIA, the agreement is not as good as it overestimates $\sigma_\theta(f)$ by about 5° for $f/f_p>2$. For low frequencies $f/f_p<1$ and slanting fetch, the performance of SWAN seems to be poor anyway. Both DIA and Xnl then predict a $\sigma_\theta(f)$ of about 15° whereas Pettersson's (2004) slanting fetch $\sigma_\theta(f)$ values , for $f/f_p<1$, are in the range of 40°–70°, of which the latter is believed to be correct (Pettersson, pers. comm., 2006).

For the mean wave directions, a marked frequency dependency was found. For high frequencies ($f/f_p>2$), the waves are roughly parallel to the wind. For low frequencies ($f/f_p<1.5$ to 2), the differences between wind and wave direction strongly depend on the wind direction and fetch geometry, while they steadily increase with decreasing frequency. The main differences between DIA and Xnl appear to occur for $f/f_p<2$, where the DIA mean wave directions tend to be much (10°–25°) closer to the wind direction than the Xnl results. As an example, Fig. 11b shows the 1D results for 130° (slanting fetch) and for 100° (wind is nearly shore-normal). The latter wind direction differs from the shore-normal winds of Figs. 10 and 11b. This is done because for shore-normal winds, the waves either propagate downwind or upwind. The former is the case for nearly all spectral components, the latter for some low-frequency components ($f/f_p<0.6$–0.8). These upwind propagating low-frequency waves are probably unphysical and result from the fact that their generation by the quadruplet interactions is insufficiently damped by the dissipation processes in SWAN.

No experimental data were found to verify the above trends, but for the evaluation of the quadruplet effects, it is instructive to compare the present data with Donelan et al.'s (1985) directional prediction method, where it is assumed that the wave direction at the peak frequency, $\theta(f_p)$, equals the direction with the longest wave component along the wind. Following Pettersson (2004), this can be implemented as:

$$\theta(f_p) = \theta|_{T_p(\theta)=\max(T_p)} \tag{13}$$

and

$$T_p(\theta) = 0.459 g^{-0.73} (U_{10}\cos(\theta-\phi))^{0.46} x(\theta)^{0.27} \tag{14}$$

where $T_p(\theta)$ is the 'peak period' of a wave component with direction θ and ϕ the wind direction. Eq. (14) is taken from Pettersson (2004) and is equivalent to our Eq. (2), except that the wind component $U_{10}(\cos(\theta-\phi))$ along the wave direction is taken, rather than U_{10} itself.

As far as the wave directions are concerned (wave heights and periods are not considered at this moment), the above is an estimate without the effect of quadruplet interactions. In Fig. 12, this estimate is compared with SWAN predictions. The results

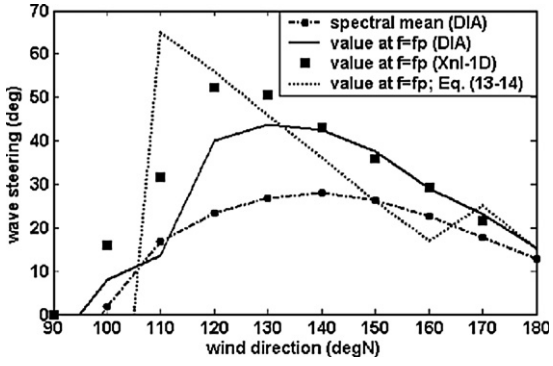

Fig. 12. Wave steering as a function of wind direction at the location FL2. Shown are the mean wave steering (SWAN-2D with DIA, dash–dot line with circles), the wave steering at the peak frequency (SWAN-2D with DIA: solid line; SWAN-1D with Xnl: black squares) and a simple estimate according to Eqs. (13) and (14) (dotted line).

for wind directions smaller than 110° are influenced too much by the kink in the coastline, but from the remainder some useful conclusions can be drawn. First it can be seen that $\theta(f_p)$ is not a good estimator for the mean wave direction as the wave steering at $f/f_p=1$ is much stronger than the mean wave steering. Secondly, for wind directions around 145° (slanting fetch) and near the spectral peak, SWAN generally predicts about 10° more wave steering than Eqs. (13) and (14). This suggests that the quadruplets indeed enhance the wave steering, as already suggested by Pettersson (2004) and in accordance with Van Vledder and Holthuijsen (1993) who suggest that in mixed wave fields, the quadruplets tend to transfer energy from the youngest to the older waves. Finally, Xnl predicts more wave steering than DIA, as in Fig. 9a.

As Xnl yields more wave steering than DIA, it would be expected that the relative magnitude of the quadruplet source term in SWAN would be larger for the Xnl-approach than for the DIA-approach. Actually, the opposite is the case. See Fig. 13, which shows the ratio of the absolute value of the quadruplet source term S_{nl4} (with the absolute values of each spectral S_{nl4}-component summed over all SWAN wave frequencies and directions) in SWAN and the net wave growth source term $S_{in}-S_{wcap}-S_{fric}$, where S_{in} is the wind input, S_{wcap} the whitecapping and S_{fric} the bottom friction. Apparently, the amount of wave steering is not only significantly influenced by the relative strength of the quadruplet interactions, but also by the directional properties of these interactions. This would imply that the type of quadruplet modelling (DIA, mDIA, Xnl, ...) and the resulting shape of the quadruplet configurations have an important influence on wave steering in spectral models. Since the trends in Fig. 13 only compare well with those in Figs. 9a and 12, it appears that the quadruplets primarily affect the wave steering, rather than the other wave variables.

Summarizing, the non-linear four-wave interactions during slanting fetch conditions mainly seem to influence the amount of wave steering, with typical effects of the order of 10°. The effect of the quadruplets on the wave heights and wave periods seems to be rather limited but it should be taken into account that it was not possible to fully deactivate the quadruplets; rather a number of different formulations were compared. The relatively limited effect of the various quadruplet formulations on H_{m0} and T_p (order 5%) also implies that even more accurate quadruplet source terms almost certainly are insufficient to obtain a full match between SWAN and the experimental data discussed in Section 4. This finding agrees with those of Ardhuin et al. (2006) who state that improvements in model performance for slanting fetch situations can only be made by simultaneous improvements in the source terms for whitecapping and wind input as well.

7. Conclusions and future research

In this paper, two main issues were discussed in relation to some crucial wave model assumptions for cases with wave growth in slanting fetch conditions. The first issue is the validity of the effective fetch concept in the use of parametric wave growth curves. The second issue is the role of the non-linear four-wave (quadruplet) interactions in relation to the choice between full spectral or directionally decoupled modelling approaches. The main conclusions for these issues are:

- For slanting and parallel fetch, the effective fetch concept as used in parametric wave growth formulas appears to be a good approximation if the distance to the coast is at least 3 km. This requirement may be relaxed to a shore-normal distance of at least 1 km if not the peak period T_p is to be predicted, but one of the spectral wave period measures (T_{m01}, T_{m-10}, T_{m02}).
- The effect of the quadruplet interactions on the wave heights and wave periods seems to be quite moderate (roughly 5%). The effect on the wave directions in slanting fetch appears to be relatively strong (about 10°); the effect on the directional spreading is rather ambiguous. This implies that for slanting fetch cases, directionally decoupled wave models with suitable wave direction estimation methods may already do quite a reasonable job.

Several other conclusions can be drawn. As for the slanting fetch phenomenon itself, we found a marked difference between high- and low-frequency waves. The former (with $f/f_p>1.5$ to 2) have the properties of locally generated wind sea, the latter are strongly influenced by the coastline. Overall, the mean wave direction in slanting fetch can deviate more than 30° from the mean wind direction (see Eq. (12)). It should be possible to evaluate most this 'wave steering' by superposition of different wave components since the quadruplet interactions appear to contribute only for about one third (10°) to this 'wave steering'.

As for the simple model approaches, the following conclusions can be drawn:

- Wave steering in slanting fetch is so strong that it has to be accounted for.
- Directional decoupling appears to be a suitable practical assumption in slanting fetch, at least when wave height and wave period errors of about 6% are acceptable, and wave direction errors of about 10°.
- For the presently available wind speed range (~10 m/s), discrepancies between various wave growth formulas for H_{m0} and T_p appear to be more critical in slanting fetch than the validity (or non-validity) of the effective fetch concept.

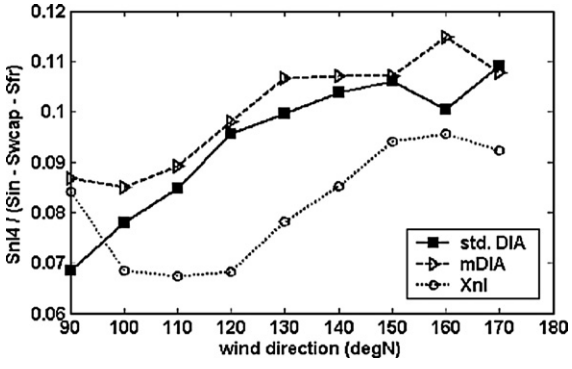

Fig. 13. SWAN-ratio of quadruplet and net wave growth source terms as a function of wind direction. Fetch and notation as in Fig. 8.

As for the latter, it is interesting to note some interesting differences between the Bretschneider (CERC, 1984) and Kahma and Calkoen (1992) formulas on one hand, and the Young and Verhagen (1996) formulas on the other hand. The former formulas have trends that agree well with SWAN, and suggest that the effective fetch concept does not hold well in slanting fetch conditions. With the Young and Verhagen (1996) formulas however, the opposite seems to be the case: slanting and parallel fetch then are the only situation where the effective fetch concept seems to hold. This suggests that the elongated shape of Lake George has led to an inadvertent tuning to slanting and parallel fetch conditions. This would imply that the present discrepancies between wave growth formulas are not only caused by wind-related factors (as investigated by Kahma and Calkoen, 1992), but also by the fetch geometry and the fetch definition of the underlying data.

As for SWAN, the following conclusions can be drawn:

- SWAN has proven to be a useful tool, not only to investigate the role of the quadruplet interactions, but also to test the effective fetch concept.
- SWAN overestimates the high-frequency tail of the spectrum and underestimates the wave periods, both with the default DIA-quadruplets and the exact Xnl-quadruplets. This suggests that the deep water source term balance needs some optimisation (new formulations) and/or retuning. The development of a saturation based white-capping formulation (Westhuysen et al., 2007) could help to solve this problem, but its applicability has still to be thoroughly tested for the very short fetches that are relevant for this type of study.
- For frequencies above the peak frequency, SWAN predicts the directional spreading quite well, especially with the Xnl-quadruplets.
- SWAN unexpectedly predicts less wave steering with DIA quadruplets than with Xnl-quadruplets, even though the quadruplet source term is weaker in the latter case. This suggests that not only the strength of the quadruplet source term influences the wave steering in slanting fetch, but also the spectral shape of the quadruplet configuration, both in terms of wave frequencies and wave directions.

As for the future research with SWAN, it is certainly useful to do some further comparisons between DIA and Xnl in order to investigate the role of the quadruplets for various wave conditions (e.g., shoaling waves, depth-limited wave growth, rapid wave growth, …). Up till recently, Xnl in SWAN had prohibitive CPU times for two-dimensional studies, but significant improvements are underway (Van Vledder, 2006).

It is important to note that a single improved source term (like Xnl) does not always lead to improved overall performance of a model (see Fig. 2 and Ardhuin et al., 2006) as model deficiencies may be masked by the retuning of other source terms. Hence, improvements in a source term should always be followed by retuning the complete wave model. The present results show rather small differences between the integral wave properties (H_{m0}, T_{m01}) obtained with DIA and Xnl, but rather large differences for the wave directional properties and wave spectra. This clearly demonstrates the importance of spectral and directional measurements for future model (re)tunings; well-documented measuring data for well-defined (not too complex) cases seem to be preferable for this.

As for the physical processes during slanting fetch, additional research is still needed. The present slanting fetch data agree well will Pettersson's (2004) data in many respects, but there is one main aspect where the data sets do not seem to agree very well. In Pettersson's (2004) data set, most slanting fetch effects seem to occur mainly for relatively old waves and large fetches ($U_{10}/c_p<2; x\sim30$ km). However, the present SWAN-data suggest that slanting fetch mainly occurs for small fetches and young waves ($x<5$ km; $U_{10}/c_p\sim4$), which is in line with recent findings of Ardhuin et al. (2006). Additional well-documented and high-quality slanting fetch data for the fetch range of 1–30 km certainly are valuable to enlarge our present insights on slanting fetch. Preferably, such data should be obtained near relatively straight shorelines and in situations without swell, currents and non-uniform wind fields. Even more important is the choice of instrumentation: directional wave measurements are needed to obtain further experimental insights in slanting fetch processes, and for a more advanced validation of wave models like SWAN (and its quadruplet formulations) in those slanting fetch conditions. However, directional measurements are not trivial for the present case because the wave periods to be measured (Fig. 2b) are very small for (directional) buoys, whereas footprint issues may play a role for other types of instruments or instrument arrays (remote sensing but also in-situ).

Additional measurement data, or further re-analyses of existing data, are also needed to quantify the range of validity (in terms of non-dimensional fetch and type of fetch geometry) for each of the Bretschneider-like wave growth formulas considered here, and elsewhere. In addition, it is highly important to make explicit the effects of various assumptions (about wind, atmospheric stability, fetch geometry, fetch definitions) that are associated with those formulas. In that way, one can hopefully resolve part of the large discrepancies between formulas as reported in Section 5 and by Kahma and Calkoen (1992) and Ris et al. (2001). This is a crucial task, because many advanced spectral models rely on simple wave growth formulas to tune their deep water source term balance. For example, SWAN is tuned to a u^*-scaled variant of the Kahma and Calkoen (1992) formulas published in Komen et al. (1994). In addition, the importance of simple wave growth formulas for practical engineering applications cannot be underestimated. This is yet another reason to make explicit all assumptions associated with those formulas, and to resolve the present discrepancies.

Acknowledgements

Rijkswaterstaat IJsselmeergebied (Lelystad, NL) is gratefully acknowledged as they provided us with the experimental data and bottom grids for Lake IJssel. Dr. Heidi Pettersson of the Finnish Institute for Maritime Research gave us helpful comments to an early draft of this paper.

References

Ardhuin, F., Herbers, T.H.C., Van Vledder, G.Ph., Watts, K.P., Jensen, R., Graber, H.C., 2006. Slanting fetch and swell effects on wind wave growth. J. Phys. Oceanogr. 37 (4), 908–931.

Booij, N., Ris, R.C., Holthuijsen, L.C., 1999. A third-generation wave model for coastal regions — model description and validation. J. Geophys. Res. 104, 7649–7666.

Bottema, M., 2007. Measured wind-wave climatology Lake IJssel (NL), Report RWS RIZA 2007.020. RWS WD, Lelystad, NL. ISBN: 9789036913997. 278 pp., http://www.rijkswaterstaat.nl/rws/riza/home/publicaties/rapporten/2007/2007_020.html.

Bottema, M., Van Vledder, G.Ph., 2005. Evaluation of the SWAN wave model in slanting fetch conditions. Proc. 5th ASCE Int. Symp. on Ocean Wave Meas. and Analysis WAVES2005, 3–7 July, Madrid, paper No. 165. 10 pp.

Bottema, M., De Waal, J.P., Regeling, H.J., 2003. Some applications of the Lake IJssel/Lake Sloten wave data set. Proc. 28th Int. Conf. Coastal Eng. Cardiff, UK, pp. 413–425.

CERC, 1984. Shore Protection Manual, US Army Coastal Engineering Research Center.

De Waal, J.P., 2001. In: Edge, B.L., Hensley, J.M. (Eds.), Wave Growth Limit in Shallow Water, Proc. 4th ASCE Int. Symp. on Ocean Wave Meas. and Analysis WAVES2001, 2–6 September, San Francisco, pp. 560–569.

Donelan, M.A., Hamilton, J., Hui, W.H., 1985. Directional spectra of wind-generated waves. Philos. Trans. Roy.Soc. London A315, 509–562.

Donelan, M.A., Skafel, M., Graber, H., Liu, P., Schwab, D., Venkatesh, S., 1992. On the growth rate of wind-generated waves. Atmos.-Ocean. 30, 457–478.

Flameling, I., 2003. In: Kosmos (Ed.), High Water, 50 Years after the 1953 Flooding Catastrophy (original Dutch title: Hoogwater, 50 jaar na de waternoodsramp). Rijkswaterstaat, The Hague (NL). ISBN: 9021539659. Utrecht (NL), 184 pp.

Hashimoto, N., Kawaguchi, K., 2001. Extension and modification of discrete interaction approximation (DIA) for computing nonlinear energy transfer of gravity wave spectra. Proc. 4th ASCE Int. Symp. on Ocean Wave Meas. and Analysis WAVES2001, 2–6 September, San Francisco, pp. 530–539.

Holthuijsen, L.H., 1983. Observations of the directional distribution of ocean-wave energy in fetch-limited conditions. J. Phys. Oceanogr. 13, 191–207.

Holthuijsen, L.H., Booij, N., Herbers, T.H.C., 1989. A prediction model for stationary short-crested waves in shallow water with ambient currents. Coast. Eng. 13, 23–54.

Kahma, K.K., Calkoen, C.J., 1992. Reconciling discrepancies in the observed growth rate of waves. J. Phys. Oceanogr. 22, 1271–1285.

Komen, G.J., Cavaleri, L., Hasselmann, K., Hasselmann, S., Janssen, P.A.E.M., 1994. Dynamics and Modelling of Ocean Waves. Cambridge University Press. 532 pp.

Pettersson, H., 2004, Wave growth in a narrow bay, PhD Thesis, Contrib. Finnish Inst. of Marine Research 09-2004.

Ris, R.C., Holthuijsen, L.C., Booij, N., 1999. A third-generation wave model for coastal regions, Part II, verification. J. Geophys. Res. 104 (C4), 7667–7681.

Ris, R., Hurdle, D.P., Van Vledder, G.Ph., Holthuijsen, L.H., 2001. Deep Water Wave Growth at Short Fetches for High Wind Speeds, Report H3817, Delft Hydraulics, Delft NL (in co-operation with Alkyon Hydraulic Consultancy & Research and Delft University of Technology).

Seymour, R.J., 1977. Estimating wave generation on restricted fetches, J. Waterway, Port, Coastal and Ocean Division. Proc. Amer. Soc. Civ. Eng. 103, 251–264.

Toffoli, A., Monbaliu, J., Lefèvre, J.M., Bitner-Gregersen, E., 2004. Dangerous sea-states for marine operations. Proc. 14th Int. Offshore and Polar Engng. Conf., Toulon, France, 23–28 May 2004, pp. 85–92.

Van Vledder, G., Holthuijsen, L.H., 1993. The directional response of ocean waves to turning winds. J. Phys. Oceanogr. 23, 177–192.

Van Vledder, G.Ph., 2006. The WRT method for the computation of non-linear four-wave interactions in discrete spectral wave models. Coast. Eng. 53, 223–242.

Westhuysen, A.J., Zijlema, M., Battjes, J.A., 2007. Nonlinear saturation-based whitecapping dissipation in SWAN for deep and shallow water. Coast. Eng. 54 (2), 151–170.

Young, I.R., 1997. The growth rate of finite depth wind-generated waves. Coast. Eng. 32, 181–195.

Young, I.R., Verhagen, L.A., 1996. The growth of fetch limited waves in water of finite depth Part 1: total energy and peak frequency. Coast. Eng. 29, 47–78.

Young, I.R., 1998. An experimental investigation of the role of atmospheric stability in wind wave growth. Coast. Eng. 34, 23–33.